Applied Microscopy
Korean Society of Microscopy

pISSN 2287-5123 · eISSN 2287-4445
http://dx.doi.org/10.9729/AM.2016.46.1.45

Regular Article

Deformation Behavior of Corrosion-Resistant Fe-Cr Alloy

Hidenori Era*, Yusuke Kono[1], Ryota Sasabuchi[1], Noriko Miyoshi[1], Tatsuya Tokunaga, Nobuya Shinozaki[2], Je-Hyun Lee[3], Toshitada Shimozaki[4]

Department Materials Science and Engineering, Kyushu Institute of Technology, Kitakyushu 804-8550, Japan
[1]Graduate School, Kyushu Institute of Technology, Kitakyushu 804-8550, Japan
[2]Department of Life Science and Systems Engineering, Kyushu Institute of Technology, Kitakyushu 808-0196, Japan
[3]School of Materials Science and Engineering, Changwon National University, Changwon 51140, Korea
[4]Engineering Research Center, Changwon National University, Changwon 51140, Korea

*Correspondence to:
Era H,
Tel: +81-93-884-3368
Fax: +81-93-884-3368
E-mail: era@post.matsc.kyutech.ac.jp

Received February 3, 2016
Revised March 14, 2016
Accepted March 14, 2016

Iron containing a high amount of chromium is known to be inferior to ductility due to σ phase formation so that it is generally difficult to apply the plastic deformation process although the alloy possesses a superior characteristics of an excellent corrosion resistance. In this study, Fe-50mass%Cr alloy was melted using high purity powder and the deformation behavior has been investigated by cold rolling and tensile test. The tensile test yielded that the alloy revealed a serration at an early stage of tensile deformation and then the serrated flow vanished to change to a normal work hardening flow at the later stage. The former was governed by twin formation process, the latter by dislocation multiplication one, bringing about a high ductility of 20% or over. The reduction ratio in cold rolling was attained as high as 90%, thus the high corrosion-resistant alloy is able to possess a high ductility.

Key Words: Iron chromium alloy, Laser melting, Deformation behavior, Corrosion resistance

INTRODUCTION

The corrosion resistance and oxidation resistance at high temperatures of iron are improved by the addition of chromium, and therefore, for example, 9 to 12 mass% Cr steels are widely applied as high temperature components in fossil-fired power plants. However, the mechanical properties such as ductility and deformability substantially decreases for Fe-Cr alloys with increasing Cr content (Maykuth & Jaffee, 1955), and this phenomenon is associated with embrittlement caused by the spinodal decomposition and by the formation of σ phase (Leslie, 1981). The properties of various alloys are affected by the presence of impurities such as carbon and nitrogen, and it has been found that the toughness of Fe-30mass%Cr alloy is degraded by these impurities (Fukuda et al., 1990). On the other hand, a highly purified Fe-50mass%Cr alloy have been reported to exhibit good ductility (Abiko, 1995), high strength and corrosion resistance (Kato et al., 1995; Takaku et al., 1995; Yokota et al., 1998). The alloy is also found to deform by dislocation slip and twinning (Kako et al., 1998). In addition to the mechanical properties, it has been reported that the formation of σ phase in Fe-Cr alloys is suppressed by purification (Tetsui et al., 1997; Yano & Abiko, 1997). In view of the reported results in previous studies, highly purified Fe-Cr alloys may be attractive for various engineering materials that require corrosion resistance and oxidation resistance. In this study, Fe-50mass%Cr alloy was laser-melted using high purity powder and the deformation behavior has been investigated by cold rolling and tensile test.

MATERIALS AND METHODS

Starting materials were powders of Fe and Cr with high purity and the sizes were under one hundred micron meters. The powders were mixed by use of attritor for 24 hours in an argon atmosphere so as to have a ratio of 50 mass% Fe and

50 mass% Cr. Chemical compositions of original and mixed powders are listed in Table 1. The original powders contained a large amount of oxygen of a few hundreds ppm because of having a relatively large surface area comparing to the mass. After mixing, the oxygen content markedly increased up to a few thousands ppm in spite of utilizing argon gas atmosphere. Other impurities were suppressed under a hundred ppm.

The mixed powder was melted by laser beam where the output power, defocused distance and scan speed were 1,500 W, 14 mm and 100 mm/min, respectively. Hereafter, the Fe-50mass%Cr alloy prepared by the above process refers to as Fe-50Cr alloy. The melted and solidified alloy was cut into a rectangular test piece. The test piece was normalized at 1,000° in centigrade for 10 minutes. A part of test piece was tried to thinner by cold rolling and the other was cut into a shape for tensile testing.

Microstructure of the alloy was investigated by means of optical microscopy, electron probe micro-analysis (EPMA), electron back scattering pattern (EBSP) analysis and transmission electron microscopy (TEM).

Table 1. Chemical compositions of Cr, Fe, and mixed powders (ppm)

	C	S	O	N	Al	Si	P	Cu	Pb	W
Cr powder	47	3	96	14	2	10	3	1	1	17
Fe powder	8	20	483	19	7	16	5	2	5	5
Mixed powder	58	1	2,135	19	8	8	4	1	7	66

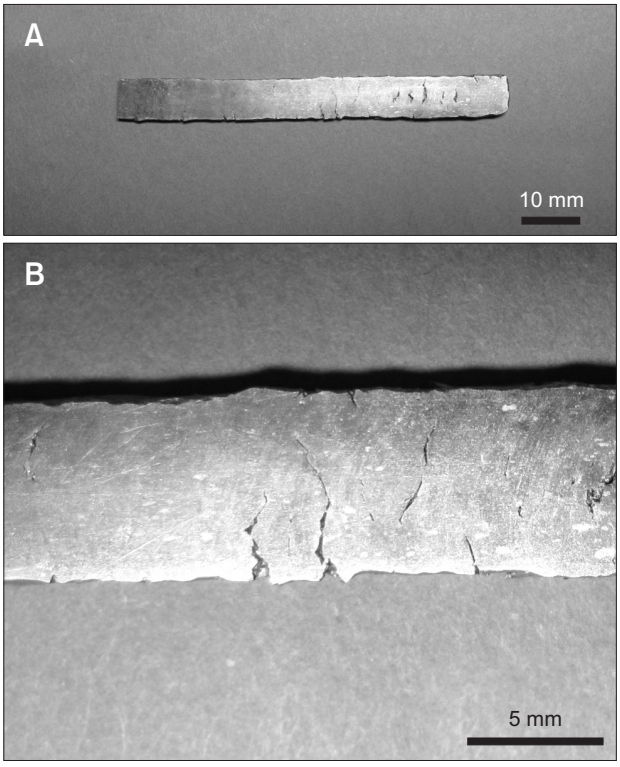

Fig. 1. (A) Appearances of cracks by cold rolling (CR: 45%) in laser-melted Fe-50Cr alloy. (B) Enlarged photo in the vicinity of the cracks.

RESULTS AND DISCUSSION

Cold Rolling

It was investigated firstly whether cold rolling can be successfully applied to the alloy without normalizing. Fig. 1 shows a photograph of the alloy cold-rolled by 45% where cracks have initiated to propagate at the middle and edge of the plate. This indicates that the alloy has a deteriorated tendency for plastic deformation. However, when the alloy was subjected to a heat treatment to normalize the structure, the alloy became recovered in deformability. As shown in Fig. 2, the alloy was successfully deformed by cold rolling where the reduction ratio attained by 90%. Another test piece was cold-rolled by 60% to obtain a square test samples for anodic polarization test and salt spray test mentioned later. It was noticed during cold rolling that the alloy emitted an acoustic phenomenon like the tin cry. This means that the alloy may reveal some inhomogeneous deformation.

Tensile Test

Fig. 3 shows results of tensile test where stress-strain curves and the corresponding acoustic emission were demonstrated. The as-solidified alloy lacked deformability to fracture at an early stage of deformation while the normalized alloy revealed a well deformability of 20% strain which is close to the value (26%) reported in a previous study (Abiko & Kato, 1998), although both of the alloys exhibited a serrated

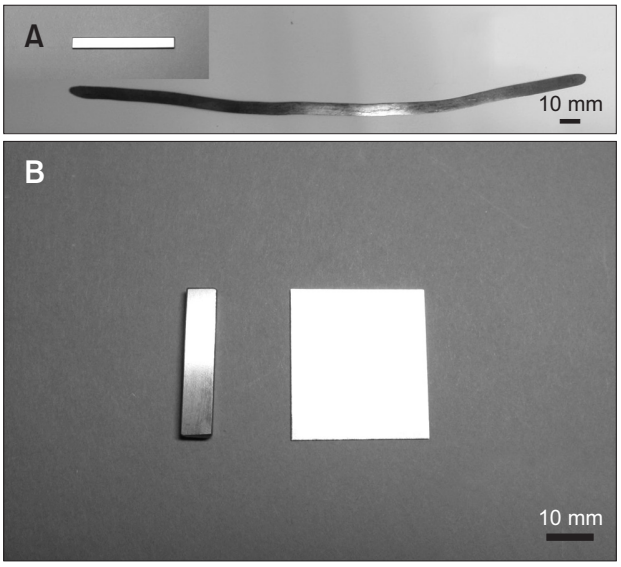

Fig. 2. Appearances after cold rolling (CR: 90%; A) and cold rolling (CR: 60%; B) for salt spray and polarization tests of Fe-50Cr alloy heat-treated at 1,000°C.

flow accompanied by acoustic emission just at an early stage of deformation up to 10%. The serrated flow and acoustic emission diminished for further deformation.

Deformation Structure

Fig. 4 shows a change in microstructure by cold rolling. There exist many black dots that may be micro voids. The micro voids were presumably introduced during melting and solidifying due to containing a large amount of oxygen. It is noteworthy that, for Fe-50Cr alloy laser-melted using high purity powder, no σ phase formation was observed by X-ray diffraction and TEM, which is consistent with previous studies showing that the formation of σ phase in Fe-Cr alloys was suppressed by purification (Tetsui et al., 1997; Yano & Abiko, 1997). After cold rolling by 2% (Fig. 4B), black lines were observed in the grains and the lines lied along some specific directions in each of the grain. Furthermore, the lines seem to terminate with grain boundary. The number of line increased with increasing the reduction ratio, as shown in Fig. 4C. This suggests that the inhomogeneous deformation is closely related to the formation of black lines.

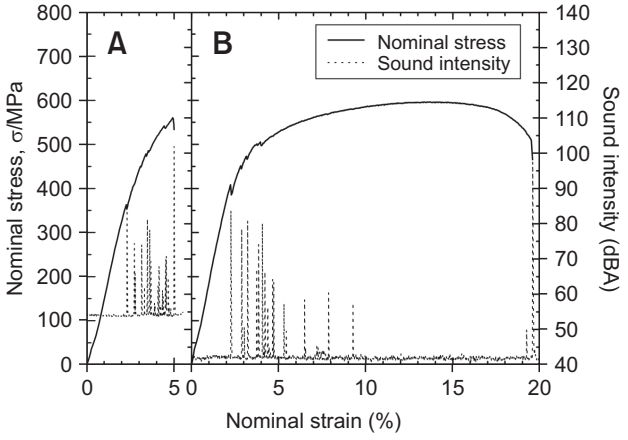

Fig. 3. Results of tensile test and acoustic measurement of as-solidified (A) and heat-treated (B) alloys.

To clarify the origin of black lines, EBSP analysis was carried out. Fig. 5 shows an orientation mapping image near a grain boundary. It is noticed that orange colored narrow bands are embedded in the blue colored matrix. The Euler angles of φ1, Φ and φ2 were acquired from the band and matrix. Then the rotational angle and axis between the band and matrix were calculated by the tensor method. The former was found to be 70.54° and latter was [101] direction, as shown in Table 2. The results yielded that the band was the deformation twin. To confirm the deformation twin, TEM observation was

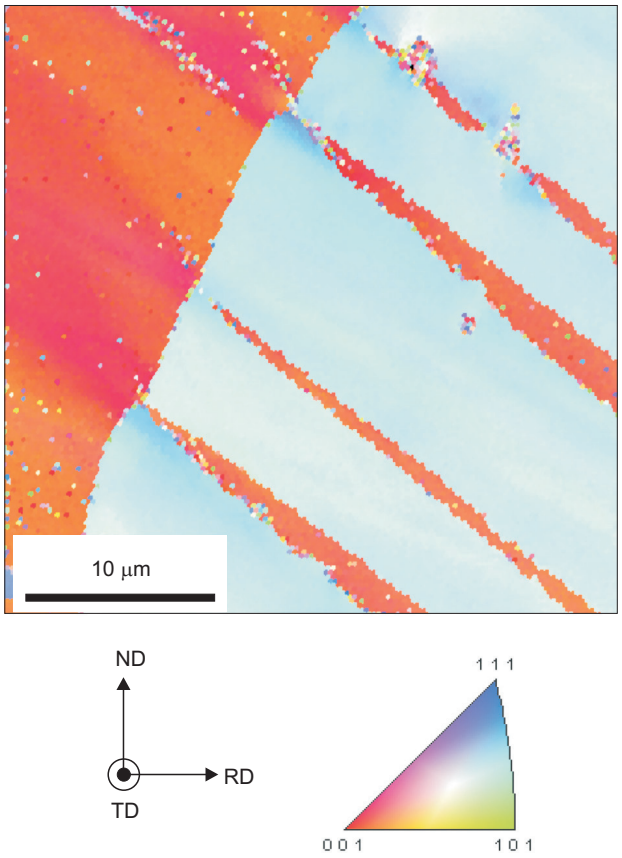

Fig. 5. Orientation mapping image after cold rolling by 5%.

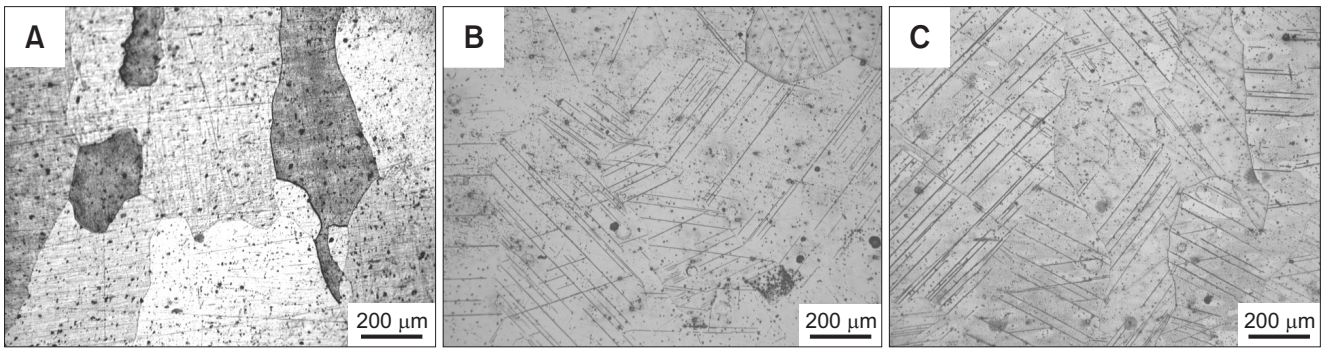

Fig. 4. Change in cross-sectional microstructure by cold rolling in heat-treated at 1,000°C (A), cold-rolled by 2% (B), and cold-rolled by 5% (C).

Table 2. Calculated results of rotational angle and rotation axis

	Euler's angle (°)			Rotational angle (°)	Rotation axis, d		
	φ_1	Φ	φ_2	θ	d_1	d_2	d_3
Matrix	181.5	7.7	199.4	70.54	0.7	0	-0.7
Band	223.0	53.0	124.2				

performed focusing on the band. As shown in Fig. 6, crystal A of matrix and crystal B of band shown in Fig. 6A has a relationship of the deformation twin that reveals in a typical bcc crystal as clarified by analysis of the diffraction pattern (Fig. 6B and C). It is clear from the results that the serrated

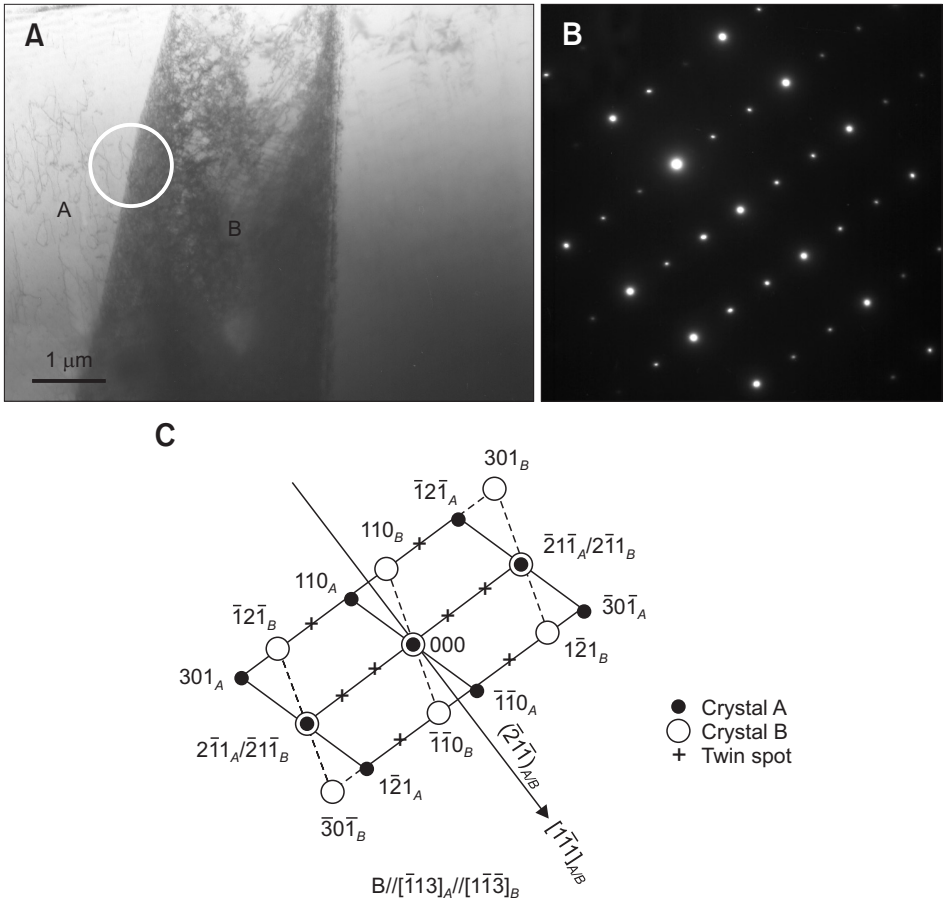

Fig. 6. Bright field image (A), selected area diffraction pattern (B), and indexed result (C) after cold rolling by 5%.

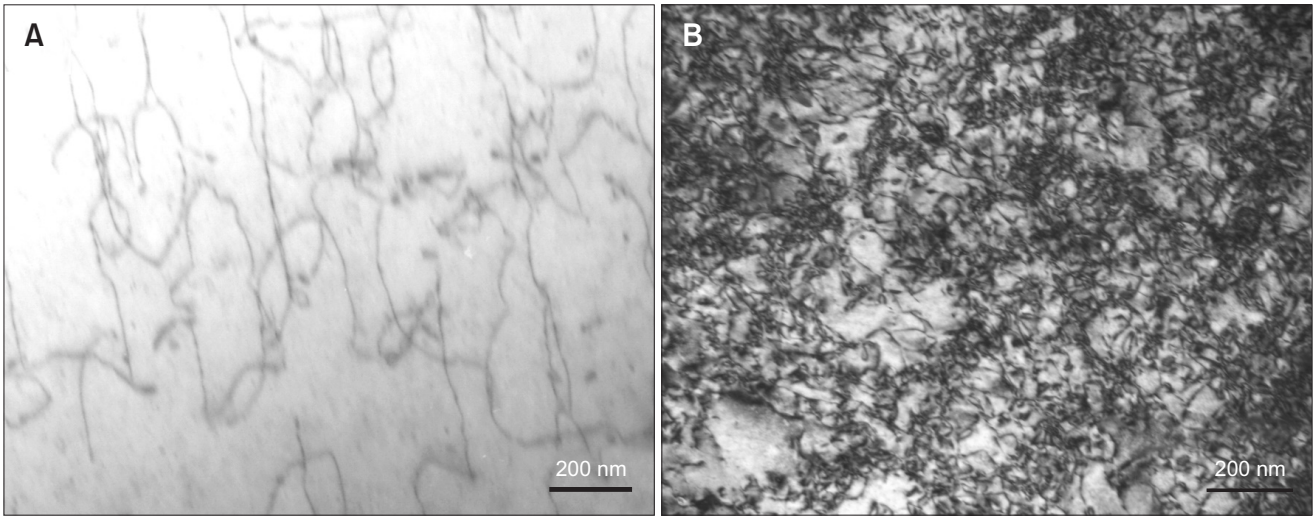

Fig. 7. Bright field images of dislocation structure in matrix at early stage (CR: 5%; A) and latter stage (CR: 11%; B) of deformation, respectively.

flow accompanied by acoustic emission and appearance of black lines are attributed to the deformation twin.
The serrated flow and acoustic emission were recognized only at an early stage of deformation. This means that the deformation at an early stage is governed by twin initiation. Fig. 7 shows a result of TEM observation focused on the matrix. Only a few dislocations were observed at a tensile strain of 5% for the alloy cold-rolled by 5% (Fig. 7A). On the other hand, dislocation had been multiplied and tangled for the alloy cold-rolled by 11% (Fig. 7B), that is, high dislocation density was brought about when stretched up to 15% which corresponds to a strain at the maximum stress (Fig. 3). Thus the deformation mode at a later stage dominates the dislocation multiplication process.

Corrosion Resistance

In order to evaluate a corrosion resistance, anodic polarization test was carried out for the cold rolled and annealed alloy plates, respectively. Ferritic stainless steel (Japanese Industrial Standards [JIS]: SUS430) and austenitic stainless steel (JIS:

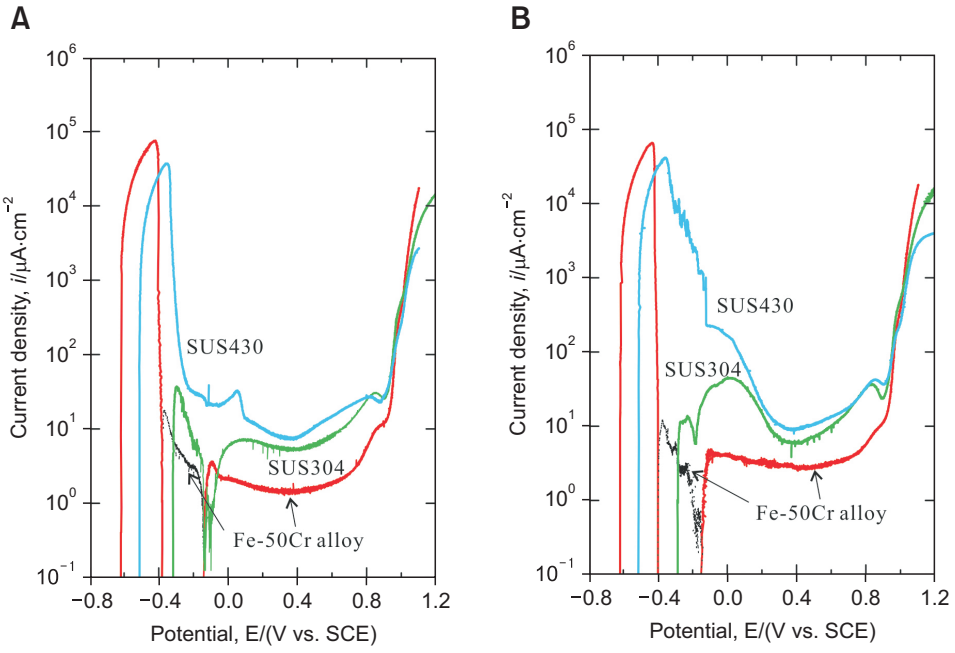

Fig. 8. Polarization curves of as-rolled (A) and subsequently annealed (B) alloys (solution: 5 mass%H_2SO_4, temperature: 30°C, sweep rate: 20 mV/min).

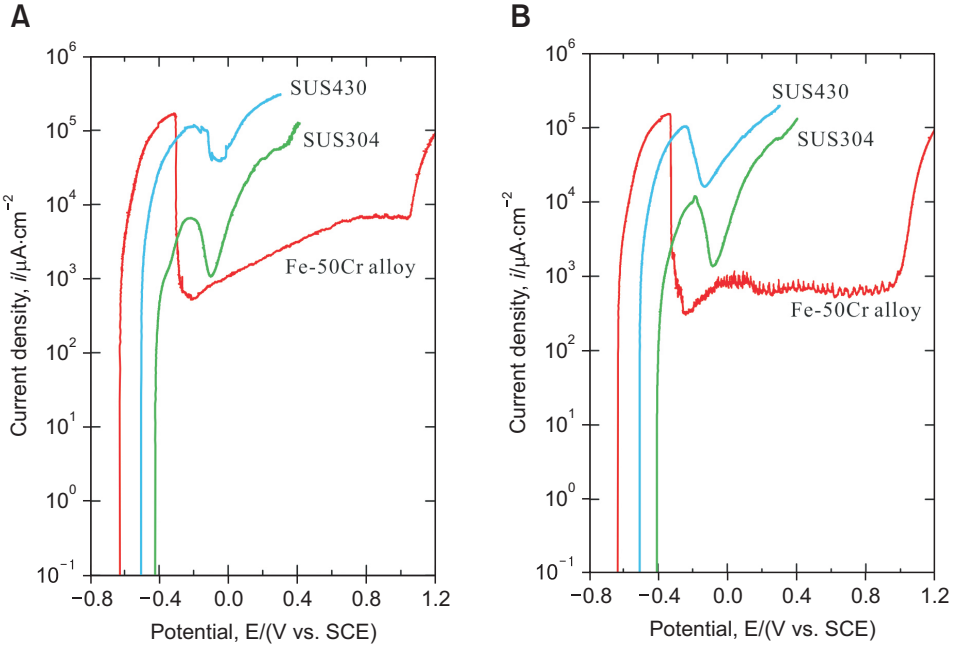

Fig. 9. Polarization curves of as-rolled (A) and subsequently annealed (B) alloys (solution: 1 N HCl, temperature: 30°C, sweep rate: 20 mV/min).

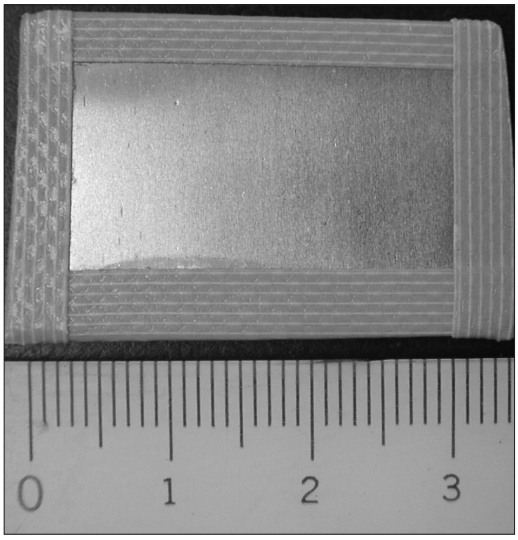

Fig. 10. Appearance of Fe-50Cr alloy sheet after salt spray test based on JIS Z 2137 (5 mass%NaCl aqueous solution) for 1,000 hours.

SUS304) were also employed as a comparison. Fig. 8 shows results of the anodic polarization test using a sulfate acid solution. In this study, cathodic current was also appeared for Fe-50Cr alloy in the potential range of about –0.4 to –0.2 V, and its absolute values are also shown as a black line in the figure. Both of the Fe-50Cr alloy plates cold rolled (Fig. 8A) and annealed (Fig. 8B) exhibited low current densities at the passivity state than SUS430 and SUS304 plates. When hydrochloric acid solution was used, the same tendency was observed as shown in Fig. 9. It is noted that the Fe-50Cr alloy plates exhibited wider potential rather than SUS430 and SUS304. Fig. 10 shows a result of salt spray test for the Fe-50Cr alloy plate. There existed no trace of corrosion but maintained almost original surface even after exposuring for 1,000 hours. These features indicate that the Fe-50Cr alloy studied here has a superior corrosion resistance compared to the conventional stainless steels.

SUMMARY

Fe-Cr alloy was melted by laser beam and solidified using high purity powders. It has been investigated for the alloy on deformability and corrosion resistance by cold rolling, tensile test, structure observation and anodic polarization test. The results are summarized as follows;
(1) Iron alloy having a high content of chromium acquired ductility in itself by laser melting followed by normalizing.
(2) Deformation proceeds through twin formation at the early stage and dislocation multiplication process at the latter.
(3) The alloy prepared in this study exhibited a superior corrosion resistance rather than conventional stainless steels in both of cold rolled or annealed state.
(4) The alloy could be applicable in usage of formable parts necessary for anti-corrosion.

CONFLICT OF INTEREST

No potential conflict of interest relevant to this article was reported.

REFERENCES

Abiko K (1995) Research on high purity Fe-Cr alloys. In: *Ultra High Purity Base Metals, Proceedings of the First International Conference on Ultra-High Purity Base Metals (UHPM-1994)*, eds. Abiko K, Hirokawa K, and Takaki S, pp. 522-523, (The Japan Institute of Metals, Sendai).

Abiko K and Kato Y (1998) Properties of a high-purity Fe-50 mass% Cr alloy. *Phys. Stat. Sol. (a)* **167**, 449-461.

Fukuda T, Kataura Y, and Ototani T (1990) Effects of carbide and nitride precipitates on mechanical properties of Fe-30%Cr alloys. *J. Jpn. Inst. Metals* **54**, 93-100.

Kako K, Isozaki S, Takaki S, and Abiko K (1998) Deformation mechanisms in high-purity Fe-50Cr(-5W) alloys at elevated temperatures. *Phys. Stat. Sol. (a)* **167**, 481-494.

Kato Y, Ujiro T, Satoh S, Yamato K, and Abiko K (1995) Influence of carbon and nitrogen on corrosion resistance of high purity Fe-50mass%Cr alloy. *J. Physique IV* **5**, C7-403-407.

Leslie W C (1981) *The Physical Metallurgy of Steels,* pp. 337-340, (McGraw-Hill, New York).

Maykuth D J and Jaffee R J (1955) *Ductile Chromium and Its Alloys*, p. 229, (ASM, Materials Park).

Takaku H, Kato S, Tani J, and Abiko K (1995) Stress corrosion cracking sensitivity of high purity Fe-Cr alloys in high temperature water. *J. Physique IV* **5**, C7-397-402.

Tetsui T, Shinohara M, and Abiko K (1997) Aging properties of ultra-high-purity Fe-High-Cr alloys. *Phys. Stat. Sol. (a)* **160**, 459-467.

Yano K and Abiko K (1997) Formation of σ phase in highly purified Fe-Cr alloys. *Phys. Stat. Sol. (a)* **160**, 449-457.

Yokota T, Satoh S, Kato Y, and Abiko K (1998) Corrosion resistance of a high purity Fe-50 mass% Cr alloy. *Phys. Stat. Sol. (a)* **167**, 495-502.